Robust Cadence Tracking for Switched FES-Cycling With an Unknown Time-Varying Input Delay

Brendon C. Allen, Christian A. Cousin, Courtney A. Rouse, and Warren E. Dixon, *Fellow, IEEE*

***Abstract*— For an individual affected by a neuromuscular condition (NC), functional electrical stimulation (FES)-induced cycling provides a means of functional restoration and therapeutic exercise. Although FES-cycling has been shown to have numerous benefits, there are challenges to implementing closed-loop FES control for coordinated motion. For example, there exists a potentially destabilizing input delay between the application (or removal) of stimulation and the resulting muscle force. Moreover, switching between multiple actuators (such as FES or motor control) can also be destabilizing. This brief develops delay-dependent switching conditions and a robust control method to account for an unknown time-varying input delay of a switched system. A Lyapunov-like analysis is performed to yield semiglobal exponential cadence tracking to an ultimate bound. Experiments were performed on six able-bodied participants and four participants with NCs to validate the developed controller. The proposed controller resulted in an average cadence error of 0.01 ± 2.00 revolutions per minute (RPM) for the able-bodied participants and 0.01 ± 2.72 RPM for participants with NCs.**

***Index Terms*— Functional electrical stimulation (FES), human–robot interaction, input delay, Lyapunov methods, rehabilitation robotics, switched systems.**

I. Introduction

NEUROLOGICAL conditions (NCs), such as traumatic brain injury (TBI), stroke, spinal cord injury (SCI), and Parkinson's disease (PD), among others, often result in a deterioration of quality of life for affected individuals [1]. A common rehabilitative exercise for individuals with lower limb NCs is closed-loop functional electrical stimulation (FES)-induced cycling [1]–[6]; however, there are several challenges associated with closed-loop FES control. The primary challenges are fatigue and the existence of an input delay, called the electromechanical delay (EMD), in response to the complex electrophysiological mechanism involved in FES-induced force production, which may result in instability [7]. Fatigue reduces the FES-induced muscle force under a fixed stimulation intensity [8] and decreases the duration an exercise can be performed (e.g., the number of repetitions), which may lower rehabilitative effectiveness. A secondary effect of fatigue is that it causes the input delay to vary [7]. Additional challenges are unmodeled disturbances and uncertain parameters in the nonlinear dynamic model [9] and nonlinearity and uncertainty of the muscle activation dynamics [10], and the coordinated functional tasks (e.g., FES cycling) require control to be switched between multiple muscle groups and often a motor to help reduce fatigue [4].

Few studies have developed FES controllers to compensate for an FES-induced input delay, and these studies have focused on continuous exercises (e.g., leg extensions) with FES of a single muscle group [11]–[13]. For example, results such as [11]–[13] all consider a continuous leg extension exercise with FES of the quadriceps femoris muscle group. The prior studies on continuous exercises only considered the contraction delay between the initial application of an electrical stimulus across a muscle and the resulting muscle contraction. When a coordinated exercise is performed, such as cycling, switching is required between multiple muscle groups and the residual forces must also be considered [14]–[18]. The residual forces result from the delayed muscle response after the removal of the electrical stimulus. Special consideration is required for these residual forces so that they are not produced by antagonistic muscles, which would increase the rate of fatigue.

Although results for with FES-induced input delays are sparse, input delayed systems have been extensively studied for general systems [19]–[34]. Often results either assume exact model knowledge (see [22]–[24]) or the input delay is known (see [24]–[26]). However, there are uncertainties in many practical engineering systems, and the input delay may be unknown and potentially time-varying (e.g., an FES-induced input delay is time-varying and difficult to measure [35]). Therefore, results such as [27]–[31] have analyzed systems with an unknown input delay. In recent years, some results have begun to examine input delay compensation for switched systems [14], [15], [32]–[34]. However, the aforementioned results do not compensate for FES-specific factors such as the development of a complex state-dependent switching signal to produce effective agonist muscle contractions despite the contraction delay while simultaneously preventing or minimizing residual antagonistic forces that remain after the stimulation has ceased.

In the authors' previous results in [14] and [15], which this work is predicated upon, closed-loop FES controllers were developed for FES-cycling. The input delay was first considered to be unknown and constant in [14] and generalized to be unknown and time-varying in [15]. Building on our

Manuscript received January 23, 2021; accepted March 22, 2021. Date of publication April 9, 2021; date of current version February 10, 2022. Manuscript received in final form March 29, 2021. This work was supported in part by NSF under Award 1762829 and in part by the Air Force Office of Scientific Research (AFOSR) under Award FA9550-18-1-0109. Recommended by Associate Editor A. Behal. *(Corresponding author: Brendon C. Allen.)*

Brendon C. Allen, Courtney A. Rouse, and Warren E. Dixon are with the Department of Mechanical and Aerospace Engineering, University of Florida, Gainesville, FL 32611 USA (e-mail: brendoncallen@ufl.edu; courtneyarouse@ufl.edu; wdixon@ufl.edu).

Christian A. Cousin is with the Department of Mechanical Engineering, The University of Alabama, Tuscaloosa, AL 35401 USA (e-mail: cacousin@eng.ua.edu).

Color versions of one or more figures in this article are available at https://doi.org/10.1109/TCST.2021.3070189.

Digital Object Identifier 10.1109/TCST.2021.3070189

precursory results in [14] and [15], this brief includes comparative experiments on six able-bodied participants and four participants with NCs (compared to no experiments in [14] and [15], less conservative gain conditions are achieved, and an extension is provided with a modified control objective (i.e., motorized assistance is continuously provided to further align with current clinical practice in rehabilitation cycles). Furthermore, a switched cadence tracking controller is developed for an FES cycle that is robust to an unknown time-varying FES-induced input delay. Trigger conditions are developed to appropriately schedule the activation and deactivation of stimulation for each muscle group and the motor such that the muscle forces occur in desired locations and the residual muscle forces are less likely to come from antagonist muscles, which would impede cycling and increase fatigue. A Lyapunov-like switched systems stability analysis is performed to prove a cadence tracking error with semiglobal exponential convergence to a uniform ultimate bound.

To demonstrate the performance of the developed controller, in-depth experiments were performed on six able-bodied participants and four participants with different NCs (spina bifida, quadriplegia, multiple sclerosis, and cerebral palsy). The experiments compare the developed controller, the extended controller, and for comparison, a controller that was developed assuming the system has no input delay. The developed controller achieved an average cadence error of 0.01 ± 2.00 revolutions per minute (RPM) for the able-bodied participants and 0.01 ± 2.72 RPM for the participants with NCs. The experimental results validate the controller and indicate that delay compensation can result in an improved FES-cycling experience when compared to a controller of the same form, but without delay compensation.

II. Model

Throughout this brief, switching signals are piecewise right-continuous and delayed functions are defined as

$$h_\tau \triangleq \begin{cases} h(t-\tau(t)), & t-\tau(t) \geq t_0 \\ 0, & t-\tau(t) < t_0 \end{cases}$$

where $t, t_0 \in \mathbb{R}_{\geq 0}$, $\tau : \mathbb{R}_{\geq 0} \to \mathbb{S}$, and $\mathbb{S} \subset \mathbb{R}_{>0}$, denote the time, initial time, EMD, and set of possible delay values [36], respectively. The nonlinear, uncertain motorized cycle-rider dynamics can be modeled as[1] [14], [15]

$$\begin{aligned} M(q)\ddot{q} + V(q,\dot{q})\dot{q} + G(q) + P(q,\dot{q}) + b_c\dot{q} + d(t) \\ = \underbrace{B_e k_e \sigma_e(q,\dot{q})}_{B_E} u_e(t) + \underbrace{\sum_{m\in\mathcal{M}} B_m(q,\dot{q},t) k_m \sigma_{m,\tau}}_{B_M^\tau(q,\dot{q},\tau,t)} u_\tau \end{aligned} \quad (1)$$

where $q : \mathbb{R}_{\geq 0} \to \mathcal{Q}$, $\dot{q} : \mathbb{R}_{\geq 0} \to \mathbb{R}$, and $\ddot{q} : \mathbb{R}_{\geq 0} \to \mathbb{R}$ denote the measurable crank angle, measurable angular velocity (cadence), and unmeasured acceleration, respectively. The set of all possible crank angles is denoted by $\mathcal{Q} \subseteq \mathbb{R}$. The inertial effects, gravitational effects, centripetal-Coriolis effects, passive viscoelastic tissue forces, disturbances, and viscous damping coefficient are denoted by $M : \mathcal{Q} \to \mathbb{R}_{>0}$, $G : \mathcal{Q} \to \mathbb{R}$, $V : \mathcal{Q} \times \mathbb{R} \to \mathbb{R}$, $P : \mathcal{Q} \times \mathbb{R} \to \mathbb{R}$, and $d : \mathbb{R}_{\geq 0} \to \mathbb{R}$ and $b_c \in \mathbb{R}_{>0}$, respectively. The unknown lumped motor and muscle control terms are denoted by $B_E \in \mathbb{R}_{>0}$ and $B_M^\tau : \mathcal{Q} \times \mathbb{R} \times \mathbb{S} \times \mathbb{R}_{\geq 0} \to \mathbb{R}_{\geq 0}$, respectively, the unknown motor and muscle effectiveness terms are denoted by $B_e \in \mathbb{R}_{>0}$ and $B_m : \mathcal{Q} \times \mathbb{R} \times \mathbb{R}_{\geq 0} \to \mathbb{R}_{>0}$, $\forall m \in \mathcal{M}$, respectively, and selectable constants are denoted by $k_e, k_m \in \mathbb{R}_{>0}$, $\forall m \in \mathcal{M}$, where $m \in \mathcal{M} \triangleq \{RH, RQ, RG, LH, LQ, LG\}$ indicates the right (R) and left (L) hamstrings (H), quadriceps femoris (Q), and gluteal (G) muscle groups. The implemented motor and FES control inputs are denoted by $u_e : \mathbb{R}_{\geq 0} \to \mathbb{R}$ and $u : \mathbb{R}_{\geq 0} \to \mathbb{R}$, respectively, and the delayed FES control input is denoted by $u_\tau : \mathbb{S} \times \mathbb{R}_{\geq 0} \to \mathbb{R}$. For a given $m \in \mathcal{M}$, the delayed FES switching signal, $\sigma_{m,\tau}$, indicates whether muscle m received the FES input u_τ at $t - \tau(t)$.

The implemented switching signals for activation of the motor and FES are denoted by $\sigma_e, \sigma_m : \mathcal{Q} \times \mathbb{R} \to \{0, 1\}$, respectively, and are defined as

$$\sigma_e(q,\dot{q}) \triangleq \begin{cases} 1, & q \in \mathcal{Q}_{\text{KDZ}} \\ 1, & q \in \mathcal{Q}_{\text{FES}}, \sum_{m\in\mathcal{M}} \sigma_m(q,\dot{q}) = 0 \\ 0, & \text{otherwise} \end{cases} \quad (2)$$

$$\sigma_m(q,\dot{q}) \triangleq \begin{cases} 1, & q_\alpha(q,\dot{q}) \in \mathcal{Q}_m \\ 1, & q_\beta(q,\dot{q}) \in \mathcal{Q}_m \, \forall m \in \mathcal{M} \\ 0, & \text{otherwise} \end{cases} \quad (3)$$

where the trigger conditions $q_\alpha, q_\beta : \mathcal{Q} \times \mathbb{R} \to \mathbb{R}$ are designed to adjust the activation/deactivation of the FES input to ensure that muscle contractions occur in desired contraction regions, defined as $\mathcal{Q}_{\text{FES}} \triangleq \bigcup_{m\in\mathcal{M}} \{\mathcal{Q}_m\}$, and to reduce/eliminate the residual torques in nondesired regions, defined as $\mathcal{Q}_{\text{KDZ}} \triangleq \mathcal{Q} \setminus \mathcal{Q}_{\text{FES}}$. To yield efficient forward pedaling (i.e., positive crank motion), each muscle's desired contraction region, denoted by $\mathcal{Q}_m \subset \mathcal{Q}$, $\forall m \in \mathcal{M}$, is defined, according to [4] as

$$\mathcal{Q}_m \triangleq \{q \in \mathcal{Q} \mid T_m(q) > \varepsilon_m\} \quad \forall m \in \mathcal{M} \quad (4)$$

where $T_m : \mathcal{Q} \to \mathbb{R}$ and $\varepsilon_m \in \mathbb{R}_{>0}$ denote a torque transfer ratio and a selectable lower threshold.

Although the parameters in (1) are unknown, the subsequently designed FES and motor controllers only require known bounds on the aforementioned parameters [4].

Property 1: The parameters in (1) can be bounded as $|d| \leq c_d$, $b_c\dot{q} \leq c_c|\dot{q}|$, $|P| \leq c_{P_1} + c_{P_2}|\dot{q}|$, $|G| \leq c_G$, $|V| \leq c_V|\dot{q}|$, and $c_m \leq M \leq c_M$, where $c_d, c_c, c_{P_1}, c_{P_2}, c_G, c_V c_m, c_M, \in \mathbb{R}_{>0}$ are known constants.

Property 2: The lumped motor (when $\sigma_e = 1$) and FES (when $\sum_{m\in\mathcal{M}} \sigma_{m,\tau} > 0$) control terms are bounded as $c_e \leq B_E \leq c_E$ and $c_b \leq B_M^\tau \leq c_B$, where $c_b, c_B, c_e, c_E \in \mathbb{R}_{>0}$ are known constants.

Property 3: The delay can be bounded as $\underline{\tau} \leq \tau \leq \bar{\tau}$, where $\underline{\tau}, \bar{\tau} \in \mathbb{R}_{>0}$ are known constants. The delay estimate error can be bounded such that $\hat{\tau} - \tau \leq \overline{\tilde{\tau}}$, where $\hat{\tau} \in \mathbb{R}_{\geq 0}$ is a constant estimate of the delay and $\overline{\tilde{\tau}} \in \mathbb{R}_{>0}$ is a known constant [36].

[1]For notational brevity, all explicit dependence on time, t, within the terms $q(t)$, $\dot{q}(t)$, $\ddot{q}(t)$, and $\tau(t)$ is suppressed.

III. Control Development

The control objective is for the bicycle crank to track a smooth desired trajectory $q_d, \dot{q}_d, \ddot{q}_d : \mathbb{R}_{\geq 0} \to \mathbb{R}$ despite the presence of uncertainties in the nonlinear dynamic model and an unknown time-varying input delay. The measurable cadence tracking error, denoted by $\dot{e} : \mathbb{R}_{\geq 0} \to \mathbb{R}$, is defined as

$$\dot{e} \triangleq \dot{q}_d - \dot{q} \tag{5}$$

where, the measurable crank position tracking error, denoted by $e : \mathbb{R}_{\geq 0} \to \mathbb{R}$, is defined as

$$e \triangleq q_d - q. \tag{6}$$

To facilitate the subsequent analysis, a measurable auxiliary tracking error, denoted by $r : \mathbb{R}_{\geq 0} \to \mathbb{R}$, is defined as

$$r \triangleq \dot{e} + \alpha_1 e + \alpha_2 e_u \tag{7}$$

where $\alpha_1, \alpha_2 \in \mathbb{R}_{\geq 0}$ are selectable constants. The auxiliary error signal, denoted by $e_u : \mathbb{R}_{\geq 0} \to \mathbb{R}$, is designed to inject a delay-free input term into the closed-loop error system and is defined as

$$e_u \triangleq -\int_{t-\hat{\tau}}^{t} u(\theta) d\theta. \tag{8}$$

The open-loop error system is obtained by taking the time derivative of (7), solving (1) for $\ddot{q}$, using (6) and (8), and adding and subtracting $M^{-1}B_M^{\tau}u_{\hat{\tau}} + e$ to obtain

$$\dot{r} = -e + \chi + M^{-1}B_M^{\tau}(u_{\hat{\tau}} - u_{\tau}) - M^{-1}B_E u_e + \left(\alpha_2 - M^{-1}B_M^{\tau}\right)u_{\hat{\tau}} - \alpha_2 u \tag{9}$$

where the auxiliary term, denoted by $\chi : \mathcal{Q} \times \mathbb{R} \times \mathbb{R}_{\geq 0} \to \mathbb{R}$, is defined as

$$\chi \triangleq \ddot{q}_d + M^{-1}(V\dot{q} + G + P + b_c\dot{q} + d) + \alpha_1\dot{e} + e.$$

By using Properties 1–6, χ can be bounded as

$$|\chi| \leq \Phi + \rho(\|z\|)\|z\| \tag{10}$$

where $\Phi \in \mathbb{R}_{>0}$ is a known constant, $\rho(\cdot)$ is a positive, strictly increasing, and radially unbounded function, and $z \in \mathbb{R}^3$ is a composite error vector defined as

$$z \triangleq \begin{bmatrix} e & r & e_u \end{bmatrix}^{\mathrm{T}}. \tag{11}$$

Based on the open-loop error system in (9) and the subsequent stability analysis, the FES and motor controller are designed, respectively, as

$$u = k_s r \tag{12}$$

$$u_e = k_1 \mathrm{sgn}(r) + (k_2 + k_3)r \tag{13}$$

where k_s, k_1, k_2, $k_3 \in \mathbb{R}_{>0}$ are selectable constants, and $\mathrm{sgn}(\cdot)$ denotes the signum function. Substituting (12) and (13) into (9) yields the closed-loop error system

$$\dot{r} = -e + \chi + k_s M^{-1}B_M^{\tau}(r_{\hat{\tau}} - r_{\tau}) - M^{-1}B_E(k_1\mathrm{sgn}(r) + (k_2 + k_3)r) + \left(\alpha_2 - M^{-1}B_M^{\tau}\right)k_s r_{\hat{\tau}} - \alpha_2 k_s r. \tag{14}$$

Lyapunov–Krasovskii functionals, denoted by $Q_1, Q_2 : \mathbb{R}_{\geq 0} \to \mathbb{R}_{>0}$, are designed to facilitate the subsequent stability analysis as

$$Q_1 \triangleq \frac{1}{2}(\varepsilon_1\omega_1 + \varepsilon_3\omega_3)k_s \int_{t-\hat{\tau}}^{t} r(\theta)^2 d\theta \tag{15}$$

$$Q_2 \triangleq \frac{\omega_2 k_s}{\hat{\tau}} \int_{t-\hat{\tau}}^{t}\int_{s}^{t} r(\theta)^2 d\theta ds \tag{16}$$

where $\varepsilon_1, \varepsilon_3, \omega_1, \omega_2, \omega_3 \in \mathbb{R}_{>0}$ are selectable constants. Based on the subsequent stability analysis, auxiliary bounding constants denoted by $\beta_1, \beta_2, \delta_1, \delta_2 \in \mathbb{R}_{>0}$ are defined as

$$\beta_1 \triangleq \min\left(\alpha_1 - \frac{\varepsilon_2\alpha_2^2}{2},\ k_s\left(\frac{1}{2}\alpha_2 - \varepsilon_1\omega_1 - \varepsilon_3\omega_3 - \omega_2\right) \frac{\omega_2}{3k_s\hat{\tau}^2} - \frac{1}{2\varepsilon_2} - \frac{\omega_3 k_s}{\varepsilon_3}\right) \tag{17}$$

$$\beta_2 \triangleq \min\left(\alpha_1 - \frac{\varepsilon_2\alpha_2^2}{2},\ \frac{c_e}{c_M}k_2 - k_s(\varepsilon_3\omega_3 + \omega_2) \frac{\omega_2}{3k_s\hat{\tau}^2} - \frac{1}{2\varepsilon_2} - \frac{\omega_3 k_s}{\varepsilon_3}\right) \tag{18}$$

$$\delta_1 \triangleq \min\left(\frac{\beta_1}{2},\ \frac{2\omega_2}{3\hat{\tau}(\varepsilon_1\omega_1 + \varepsilon_3\omega_3)},\ \frac{1}{3\hat{\tau}}\right) \tag{19}$$

$$\delta_2 \triangleq \min\left(\frac{\beta_2}{2},\ \frac{2\omega_2}{3\hat{\tau}(\varepsilon_1\omega_1 + \varepsilon_3\omega_3)},\ \frac{1}{3\hat{\tau}}\right) \tag{20}$$

where $\varepsilon_2 \in \mathbb{R}_{>0}$ is a selectable constant.

IV. Stability Analysis

In the subsequent analysis, switching times are denoted by $\{t_n^i\}$, $i \in \{m, e\}$, $n \in \{0, 1, 2, \ldots\}$, which denote the instants in time when B_M^{τ} becomes nonzero ($i = m$) and when B_M^{τ} becomes zero ($i = e$). A positive definite, continuously differentiable, common Lyapunov function candidate that is defined on a domain $\mathcal{D} \subseteq \mathbb{R}^5$ and denoted by $V_L : \mathcal{D} \to \mathbb{R}_{>0}$ is defined as

$$V_L \triangleq \frac{1}{2}e^2 + \frac{1}{2}r^2 + \frac{1}{2}\omega_3 e_u^2 + Q_1 + Q_2 \tag{21}$$

which satisfies the following inequalities:

$$\lambda_1\|y\|^2 \leq V_L \leq \lambda_2\|y\|^2 \tag{22}$$

where $y \in \mathbb{R}^5$ is defined as

$$y \triangleq \begin{bmatrix} z^{\mathrm{T}} & \sqrt{Q_1} & \sqrt{Q_2} \end{bmatrix}^{\mathrm{T}} \tag{23}$$

and $\lambda_1, \lambda_2 \in \mathbb{R}_{>0}$ are known constants defined as

$$\lambda_1 \triangleq \min\left(\frac{1}{2}, \frac{\omega_3}{2}\right), \quad \lambda_2 \triangleq \max\left(1, \frac{\omega_3}{2}\right).$$

For the subsequent stability analysis, let the set of initial conditions be defined as

$$S_{\mathcal{D}} \triangleq \left\{ y \in \mathcal{D} \mid \|y\| < \sqrt{\frac{\lambda_1}{\lambda_2}}\gamma \right\} \tag{24}$$

where $\gamma \in \mathbb{R}_{>0}$ is a known constant and is defined as[2] $\gamma \triangleq \inf\{\rho^{-1}((\sqrt{\kappa}, \infty))\}$, where $\kappa \triangleq \min((1/2)\beta_1\alpha_2 k_s, (2c_e/c_M)k_3\beta_2)$.

[2]For a set A, the inverse image is defined as $\rho^{-1}(A) \triangleq \{a \mid \rho(a) \in A\}$.

Theorem 1: The closed-loop error system in (14) is uniformly ultimately bounded in the sense that

$$\|y(t)\|^2 \leq \frac{\lambda_2}{\lambda_1}\|y(t_0)\|^2 \exp(-\lambda_3(t-t_0)) + \frac{\upsilon}{\lambda_1\lambda_3}(1-\exp(-\lambda_3(t-t_0))) \quad (25)$$

where $\upsilon \triangleq (1/\alpha_2 k_s)(\Phi + k_s\bar{\tilde{\tau}}\Upsilon(c_B/c_m))^2$, $\Upsilon \in \mathbb{R}_{>0}$ is a known constant and $\lambda_3 \triangleq \lambda_2^{-1}\min(\delta_1, \delta_2)$, $\forall t \in [t_0, \infty)$, provided $y(t_0) \in S_{\mathcal{D}}$, and the following gain conditions are satisfied:

$$\alpha_1 > \frac{\varepsilon_2\alpha_2^2}{2},\ \alpha_2 > 2(\varepsilon_1\omega_1 + \varepsilon_3\omega_3 + \omega_2) \quad (26)$$

$$\omega_2 > 3k_s\hat{\tau}^2\left(\frac{1}{2\varepsilon_2} + \frac{\omega_3 k_s}{\varepsilon_3}\right),\quad \sqrt{\lambda_1^{-1}\lambda_3^{-1}\upsilon} < \gamma \quad (27)$$

$$k_1 \geq \frac{c_M}{c_e}(\Phi + k_s\Upsilon\hat{\tau}|\alpha_2 - \varepsilon_1\omega_1|) \quad (28)$$

$$k_2 > \frac{k_s c_M}{c_e}(\varepsilon_3\omega_3 + \omega_2),\quad k_3 > 0 \quad (29)$$

$$\max\left(\left|\alpha_2 - \frac{c_b}{c_M}\right|, \left|\alpha_2 - \frac{c_B}{c_m}\right|\right) \leq \varepsilon_1\omega_1. \quad (30)$$

Proof: The proof follows from the development in [15]. ■

V. Extension

An extension of the developed controllers in (12) and (13) to improve the gain conditions is to allow for the motor to always be activated. This change is reflected by modifying the motor switching condition from (2) to $\sigma_e(q, \dot{q}) \triangleq 1$.

For comparative purposes, an additional controller/switching signal combination can be created to compensate for the system dynamics in (1) if the FES input delay was considered to be negligible. This "delay-free" controller can be generated by removing the delay-compensating term e_u from the auxiliary tracking error system in (7), such that $r \triangleq \dot{e} + \alpha_1 e$, and using (12) and (13) with this modified error system. In addition, since the delay is assumed to be negligible, the switching signals do not need to compensate for the delay and can be defined as

$$\sigma_m(q) \triangleq \begin{cases} 1, & q \in \mathcal{Q}_m \\ 0, & \text{otherwise} \end{cases},\quad \sigma_e(q) \triangleq \begin{cases} 1, & q \in \mathcal{Q}_{\text{KDZ}} \\ 0, & \text{otherwise} \end{cases} \quad (31)$$

such as in [4]. The stability analysis for the delay-free controller can be developed using a method similar to [4].

VI. Experiment

The performance of the developed controllers and switching signals in (2), (3), (12), and (13), henceforth collectively labeled as Controller A, was validated through experiments on both able-bodied participants and participants with NCs. To better examine the performance of Controller A compared to alternative cadence tracking controllers, the extension and delay-free controllers described in Section V were implemented, henceforth labeled as Controllers B and C, respectively. To allow for the best comparison, all three controllers were designed to have the same form and the same objective of cadence tracking. By comparing the three controllers, insights are provided on the effect of delay compensation and the effect of switching the motor ON and OFF.

TABLE I
Participant Demographics

Participant	Age	Sex	Condition	Time Since Diagnosis
P1	24	M	None	- -
P2	26	M	None	- -
P3	21	F	None	- -
P4	24	M	None	- -
P5	22	F	None	- -
P6	24	M	None	- -
N1	26	M	Spina Bifida (L5-S1)	26yr
N2	58	M	Quadriplegia	5yr
N3	57	F	Multiple Sclerosis	10yr
N4	42	F	Cerebral Palsy	42yr

TABLE II
Comparative Results for Able-Bodied and Neurological Population During Steady-State Operation: Reported as Average±Standard Deviation

Controller	Participant	Cadence Error (RPM)	Motor Input (A)*	FES Input (μs)†	FES on time (%)‡
A	P1	0.06±2.16	1.60±0.13	60.97±3.40	63.71
	P2	0.06±2.66	1.94±0.29	78.54±6.82	65.19
	P3	0.05±2.38	1.65±0.15	76.64±3.97	65.95
	P4	-0.04±1.40	1.15±0.13	36.61±2.52	66.32
	P5	-0.02±1.86	1.50±0.12	31.85±1.58	67.91
	P6	-0.03±1.53	1.39±0.09	21.74±0.46	72.44
	Average	**0.01±2.00**	**1.54±0.15**	**51.06±3.12**	**66.92**
	N1	0.00±2.10	1.32±0.09	40.28±1.92	74.96
	N2	0.00±2.70	1.87±0.13	224.25±12.51	73.54
	N3	0.03±2.96	2.01±0.16	52.43±2.39	72.61
	N4	0.00±3.14	1.84±0.13	36.39±2.39	74.90
	Average	**0.01±2.72**	**1.76±0.13**	**88.34±4.81**	**74.00**
B	P1	0.01±1.27	1.73±0.14	51.04±3.44	64.02
	P2	0.05±1.52	2.05±0.26	63.79±6.95	66.21
	P3	0.03±1.22	1.86±0.15	64.05±4.16	66.50
	P4	-0.03±0.80	1.14±0.13	37.61±2.28	65.15
	P5	-0.01±1.25	1.62±0.15	30.36±1.57	68.09
	P6	-0.02±0.66	1.41±0.08	20.83±0.30	72.85
	Average	**0.00±1.12**	**1.64±0.15**	**44.61±3.12**	**67.14**
	N1	-0.03±0.87	1.30±0.08	30.98±1.12	75.43
	N2	-0.04±1.08	1.89±0.11	146.28±7.67	74.12
	N3	-0.02±0.93	2.04±0.15	39.05±2.25	73.90
	N4	-0.05±1.34	1.88±0.12	30.91±0.87	76.38
	Average	**-0.04±1.06**	**1.78±0.12**	**61.80±2.98**	**74.96**
C	P1	0.09±3.29	1.61±0.14	75.31±5.26	43.15
	P2	0.10±3.86	1.87±0.27	83.78±5.91	39.11
	P3	0.09±3.68	1.78±0.21	82.66±3.63	38.70
	P4	-0.03±1.93	1.04±0.11	35.91±3.08	48.65
	P5	-0.02±2.32	1.53±0.12	34.03±1.14	45.58
	P6	0.00±2.00	1.40±0.09	24.12±0.23	62.39
	Average	**0.04±2.85**	**1.54±0.16**	**55.97±3.25**	**46.26**
	N1	-0.02±2.70	1.27±0.10	44.87±2.13	49.17
	N2	0.23±6.72	5.55±0.93	345.80±16.83	44.23
	N3	0.08±4.11	2.05±0.26	67.09±4.91	49.30
	N4	0.08±3.97	1.87±0.16	41.57±1.47	43.05
	Average	**0.09±4.37**	**2.69±0.36**	**124.83±6.33**	**46.44**

*For post-processing, a single crank-cycle (a moving window of approximately 1.2 seconds) averaging filter was applied on the motor input.
†The average and standard deviation of the applied stimulation was calculated using the maximum stimulation delivered to each muscle group for each FES region.
‡This variable represents the average percentage of a single crank cycle that FES was applied to at least one of the muscle groups.

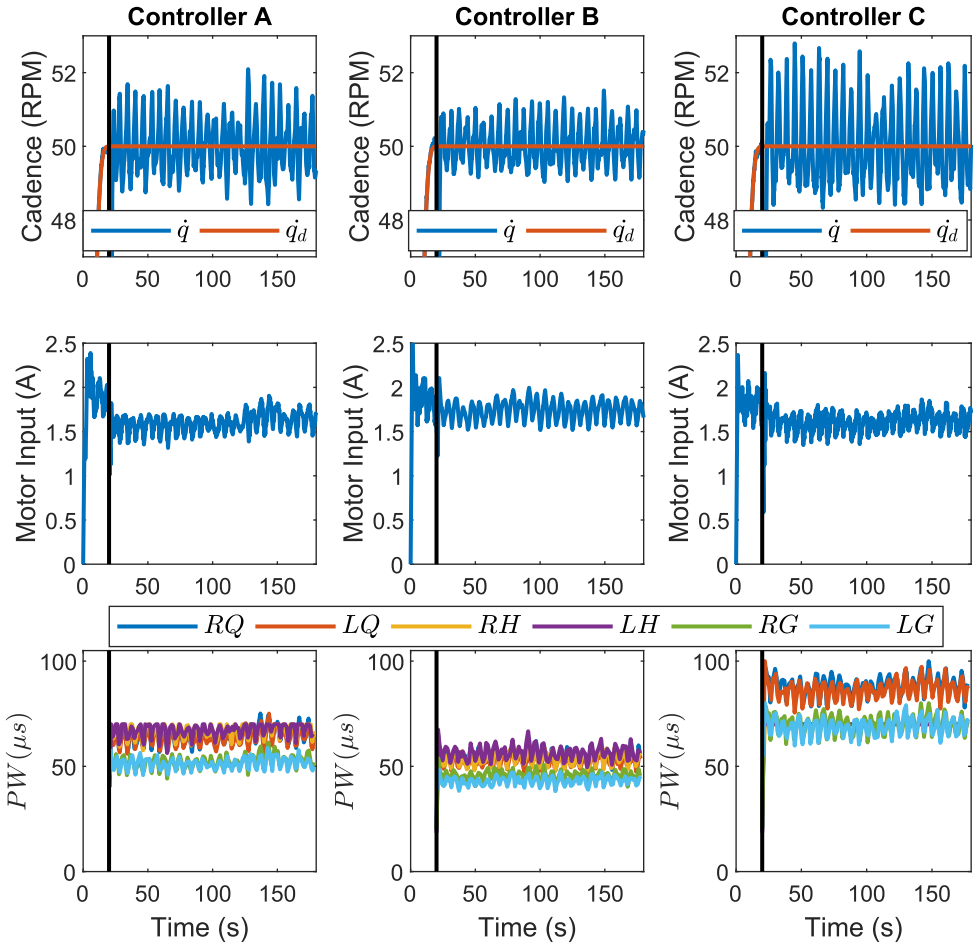

Fig. 1. Desired versus the filtered cadence (top), filtered motor input (middle), and the peak FES input PW for each FES region applied to the right (R) and left (L) quadriceps (Q), hamstring (H), and gluteal (G) (bottom) are depicted for Controllers A, B, and C from left to right for participant P1. Vertical black line indicates the time when steady-state was reached. A 1.2 s moving average filter was used on the actual cadence and the motor input for visual clarity.

A. Experimental Testbed

The experimental testbed consisted of a modified recumbent tricycle (TerraTrike Rover) mounted on a trainer and riser rings to make it stationary as described in [1] and [4]. A desktop computer executing MATLAB/Simulink/Quarc was used to interface the encoder (US Digital H1), motor (Unite Motor Company), and stimulator (Hasomed Rehastim) through a data acquisition board (Quanser Q-PIDe) at 500 Hz. Similar to [1], the current amplitude (90, 80, and 70 mA for the quadriceps, hamstrings, and gluteals, respectively) and stimulation frequency (60 Hz) of the stimulator was fixed, while the pulsewidth (PW) was used as the control input in (12).

B. Experimental Methods

An experimental protocol was performed on six able-bodied participants and four participants with NCs. The demographic information for each participant is shown in Table I.

Able-bodied participants are referred to by the letter "P" followed by their participant number, while participants with neurological conditions are referred to by the letter "N" followed by their participant number. Each participant gave written informed consent approved by the University of Florida Institutional Review Board. During the experiment, each participant was instructed to relax and make no volitional effort to either assist or resist the FES or electric motor input (i.e., to be a passive rider, blind to the desired or actual trajectory). The experiment was repeated three times for each participant with the only change being the implemented controller. Controllers A, B, and C were implemented in a random order for the experiment. To further limit the effect of fatigue, rest of at least 5 min was provided between each experiment.

Before the experiments began, the electrodes (Axelgaard ValuTrode CF7515) were placed on each muscle group (quadriceps, hamstrings, and gluteals) and the participant was seated on the cycle with their feet secured using orthotic boots (Össur Rebound Air Tall). The seat was adjusted to ensure the participant's comfort while cycling. Measurements as detailed in [4] were performed to determine the desired FES regions of the crank for each participant. The cycle was then run at 50 RPM, and open-loop stimulation was applied to one muscle group at a time to determine a comfort limit for each muscle, called the comfort threshold. If during an experiment, the participants comfort threshold was reached, the stimulation was saturated.

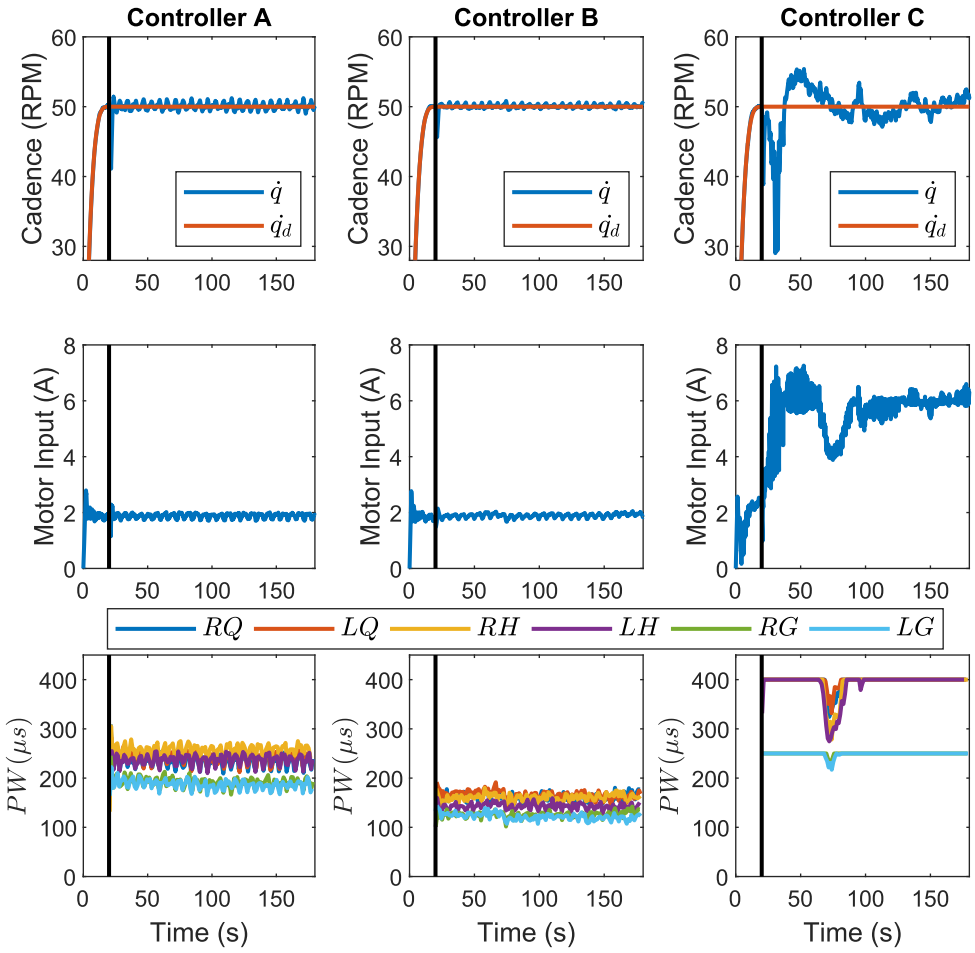

Fig. 2. Desired versus the filtered cadence (top), filtered motor input (middle), and the peak FES input PW for each FES region applied to the right (R) and left (L) quadriceps (Q), hamstring (H), and gluteal (G) (bottom) are depicted for Controllers A, B, and C from left to right for participant N2. Vertical black line indicates the time when steady state was reached. A 1.2 s moving average filter was used on the actual cadence and the motor input for visual clarity.

The experimental protocol lasted 180 s. The first 20 s consisted of the motor tracking a smooth cadence ramp from zero to $\dot{q}_d = 50$ RPM, at which point either Controller A, B, or C was implemented for the remainder of the experiment. The goal of the remaining 160 s of the experiment was to track a constant desired cadence of 50 RPM, similar to [1]. This protocol was repeated for each controller.

VII. Results

Experiments were conducted using Controllers A, B, and C on both able-bodied participants and those with NCs. Each controller was implemented on each participant for a single trial. The demographics of the four neurological participants are shown in Table I. Participant N2 has quadriplegia and felt little sensation in his limbs resulting in higher stimulation thresholds. Participants N1, N3, and N4 were more sensitive to the stimulation resulting in lower stimulation thresholds, with Participant N4 being the most sensitive. Experiments were performed on participants with a range of NCs to demonstrate each controller's stability over a range of rider capabilities.

The cadence error, motor input, and FES input for both populations are shown in Table II. To highlight the performance of Controllers A, B, and C, the cadence tracking results and control inputs over the entire experiment are shown in Figs. 1 and 2 for Participants P1 and N2, respectively. Typical results for both populations are represented by the results of Participant P1. The results of Participant N2 are also depicted because his results deviated from that of Participant P1 and because he is quadriplegic and unable to provide volitional effort; thus, any muscle produced force is caused solely due to the controllers.

VIII. Discussion

The experimental results conducted on both able-bodied and neurologically impaired populations demonstrate the validity of Controller A in tracking cadence despite uncertainties in the system and an unknown time-varying input delay, as shown in Figs. 1 and 2. In fact, for the able-bodied participants, the average standard deviation of the cadence tracking error was less than 3 RPM for each controller, as shown in Table II. For the participants with NCs, Controllers A and B outperformed Controller C in cadence tracking, as shown in Table II and Fig. 2. Controller B had the best cadence tracking as shown in Table II because Controller B maintained motor control throughout the experiment. Controller B was designed to achieve the best possible tracking performance by the

controllers in (12) and (13). Controller C had the largest standard deviations for cadence tracking errors (Table II).

For Participants P1 and N2, the FES and motor inputs across the experiment for each controller are shown in Figs. 1 and 2. From Table II and Figs. 1 and 2, it is clear that Controller C required higher FES inputs than Controllers A and B. In fact, for able-bodied participants, Controllers B and C had average peak FES inputs that were 12.6% lower and 9.6% higher than Controller A, respectively. For participants with an NC, Controllers B and C had average peak FES inputs that were 30.0% lower and 41.3% higher than Controller A, respectively. Therefore, it can be noted that Controller B tends to decrease the required FES input. However, for each participant, Table II indicates that on average, the FES is on 69.8%, 70.3%, and 46.3% of the time for Controllers A, B, and C, respectively. Thus, Controller C increased the FES input, but the FES is on for a shorter amount of time. Although the FES duration is shorter for Controller C, participants commonly indicated that Controller C felt less comfortable because it resulted in higher FES inputs when compared to Controllers A and B.

For each participant, the average motor input for each controller is shown in Table II. For the able-bodied participants, the motor input was 6.5% higher for Controller B when compared to Controller A and C. For participants with an NC, the motor input was about 53% higher for Controller C than for Controllers A and B. Overall, the differences between motor input for each participant and controller were fairly similar, with the exception of the much larger input for Participant N2 and Controller C. This result is noteworthy because, although the motor is on the least for Controller C, as shown in Table II, the average motor input over one cycle was about the same for each controller. Since Participant N2 had poor cadence tracking with Controller C, the motor required much larger inputs to maintain the stability of the system.

Controller C on average had larger cadence tracking errors and higher FES inputs when compared to Controllers A and B, resulting in the worst performance. In addition, for Participant N2, Controller C resulted in the largest overall tracking errors and highest motor and FES inputs (see Table II). Controller C does not account for the delay, which results in the muscle contractions starting too late and thus occurring in less efficient regions of the crank cycle, contributing to the poor tracking performance relative to Controllers A and B. Controller B had the best tracking performance; however, in general, it caused the FES inputs to be lower than the other controllers. The challenge with Controller B is that the motor is always active, as is often the case in current clinical practice, and both the motor and FES have the same cadence tracking control objective. Therefore, it is possible that for some participants, the FES may be too low to even elicit muscle contractions since the tracking could solely be achieved by the motor. FES has been shown to be beneficial for rehabilitation and it is desired for the participant to contribute as much as possible [1], [4], [5]. Controller A, although it did not perform as well as Controller B, had much better tracking than Controller C and resulted, on average, in more FES being applied than Controller B while still being at a comfortable level. In fact, for the participants with NCs in Table II, the standard deviation of the cadence error, average motor input, and average peak FES input is 60.7%, 52.8%, and 41.3% larger, respectively, for Controller C than Controller A.

IX. Conclusion

In this brief, delay-dependent switching conditions and robust cadence tracking controllers are developed for a switched uncertain nonlinear dynamic system in the presence of bounded unknown additive disturbances and an unknown time-varying input delay. A Lyapunov-like stability analysis was performed on the proposed controllers, which guarantees semiglobal exponential tracking to an ultimate bound. An extension of the proposed controller is provided to maintain motor control throughout the crank cycle (as opposed to switching the motor ON and OFF), and for comparison, a third controller was developed assuming that the system had no input delay. Experiments were performed on six able-bodied participants and four participants with NCs to compare the performance of these three controllers. The results indicate that the proposed controller exhibited the desired performance of cadence tracking with FES contributions with an average cadence error of 0.01 ± 2.00 RPM for the able-bodied participants and 0.01 ± 2.72 RPM for participants with NCs. Future work will seek to develop a dual objective control system, where the motor will track the cadence for all time (to take advantages of the motor always being ON), while power or torque will be tracked by a delay-compensating FES controller (to ensure that the muscles are contributing). Additional work includes the development of adaptive control methods to either estimate the EMD or to otherwise provide compensation for the EMD. Furthermore, clinical trials can be performed to further validate the clinical impacts of compensating for the EMD or closed-loop FES control in general.

Acknowledgment

Any opinions, findings and conclusions, or recommendations expressed in this material are those of the author(s) and do not necessarily reflect the views of the sponsoring agency.

References

[1] C. A. Cousin, C. A. Rouse, V. H. Duenas, and W. E. Dixon, "Controlling the cadence and admittance of a functional electrical stimulation cycle," *IEEE Trans. Neural Syst. Rehabil. Eng.*, vol. 27, no. 6, pp. 1181–1192, Jun. 2019.

[2] D. J. Pons, C. L. Vaughan, and G. G. Jaros, "Cycling device powered by the electrically stimulated muscles of paraplegics," *Med. Biol. Eng. Comput.*, vol. 27, no. 1, pp. 1–7, Jan. 1989.

[3] L. M. Schutte, M. M. Rodgers, F. E. Zajac, and R. M. Glaser, "Improving the efficacy of electrical stimulation-induced leg cycle ergometry: An analysis based on a dynamic musculoskeletal model," *IEEE Trans. Rehabil. Eng.*, vol. 1, no. 2, pp. 109–125, Jun. 1993.

[4] M. J. Bellman, R. J. Downey, A. Parikh, and W. E. Dixon, "Automatic control of cycling induced by functional electrical stimulation with electric motor assistance," *IEEE Trans. Autom. Sci. Eng.*, vol. 14, no. 2, pp. 1225–1234, Apr. 2017.

[5] C. A. Cousin *et al.*, "Closed-loop cadence and instantaneous power control on a motorized functional electrical stimulation cycle," *IEEE Trans. Control Syst. Technol.*, vol. 28, no. 6, pp. 2276–2291, Nov. 2020.

[6] C. A. Cousin, P. Deptula, C. A. Rouse, and W. E. Dixon, "A switched Lyapunov-passivity approach to motorized FES cycling using adaptive admittance control," *IEEE Trans. Control Syst. Technol.*, to be published.

[7] R. J. Downey, M. Merad, E. J. Gonzalez, and W. E. Dixon, "The time-varying nature of electromechanical delay and muscle control effectiveness in response to stimulation-induced fatigue," *IEEE Trans. Neural Syst. Rehabil. Eng.*, vol. 25, no. 9, pp. 1397–1408, Sep. 2017.

[8] J. Ding, A. S. Wexler, and S. A. Binder-Macleod, "A predictive fatigue model. I. Predicting the effect of stimulation frequency and pattern on fatigue," *IEEE Trans. Neural Syst. Rehabil. Eng.*, vol. 10, no. 1, pp. 48–58, Mar. 2002.

[9] Z. Li, M. Hayashibe, C. Fattal, and D. Guiraud, "Muscle fatigue tracking with evoked EMG via recurrent neural network: Toward personalized neuroprosthetics," *IEEE Comput. Intell. Mag.*, vol. 9, no. 2, pp. 38–46, May 2014.

[10] E. S. Idsø, T. Johansen, and K. J. Hunt, "Finding the metabolically optimal stimulation pattern for FES-cycling," in *Proc. Conf. Int. Funct. Electr. Stimulation Soc.*, Bournemouth, U.K., Sep. 2004, pp. 239–241.

[11] N. Sharma, C. M. Gregory, and W. E. Dixon, "Predictor-based compensation for electromechanical delay during neuromuscular electrical stimulation," *IEEE Trans. Neural Syst. Rehabil. Eng.*, vol. 19, no. 6, pp. 601–611, Dec. 2011.

[12] I. Karafyllis, M. Malisoff, M. D. Queiroz, M. Krstic, and R. Yang, "Predictor-based tracking for neuromuscular electrical stimulation," *Int. J. Robust Nonlinear Control*, vol. 25, no. 14, pp. 2391–2419, Sep. 2015.

[13] S. Obuz, R. J. Downey, A. Parikh, and W. E. Dixon, "Compensating for uncertain time-varying delayed muscle response in isometric neuromuscular electrical stimulation control," in *Proc. Amer. Control Conf. (ACC)*, Jul. 2016, pp. 4368–4372.

[14] B. C. Allen, C. A. Cousin, C. A. Rouse, and W. E. Dixon, "Cadence tracking for switched FES cycling with unknown input delay," in *Proc. IEEE 58th Conf. Decis. Control (CDC)*, Nice, France, Dec. 2019, pp. 60–65.

[15] B. Allen, C. Cousin, C. Rouse, and W. E. Dixon, "Cadence tracking for switched FES-cycling with unknown time-varying input delay," in *Proc. ASME Dyn. Syst. Control Conf.*, Oct. 2019, pp. 1–7.

[16] B. C. Allen, K. Stubbs, and W. E. Dixon, "Robust cadence tracking for switched FES-cycling with an unknown time-varying input delay using a time-varying estimate," in *Proc. IFAC World Congr.*, 2020.

[17] B. C. Allen, K. J. Stubbs, and W. E. Dixon, "Robust power and cadence tracking on a motorized FES cycle with an unknown time-varying input delay," in *Proc. 59th IEEE Conf. Decis. Control (CDC)*, Dec. 2020, pp. 3407–3412.

[18] B. C. Allen, K. J. Stubbs, and W. E. Dixon, "Saturated control of a switched FES-cycle with an unknown time-varying input delay," in *Proc. IFAC Conf. Cyber-Phys. Hum.-Syst.*, 2020.

[19] M. Krstic, *Delay Compensation for Nonlinear, Adaptive, and PDE Systems*. Boston, MA, USA: Springer, 2009.

[20] L. Karafyllis and M. Krstic, *Predictor Feedback for Delay Systems: Implementations and Approximations*. Springer, 2017.

[21] J.-P. Richard, "Time-delay systems: An overview of some recent advances and open problems," *Automatica*, vol. 39, no. 10, pp. 1667–1694, Oct. 2003.

[22] N. Bekiaris-Liberis and M. Krstic, "Compensation of time-varying input and state delays for nonlinear systems," *J. Dyn. Syst., Meas., Control*, vol. 134, no. 1, Jan. 2012, Art. no. 011009.

[23] F. Mazenc, S.-I. Niculescu, and M. Bekaik, "Stabilization of time-varying nonlinear systems with distributed input delay by feedback of plant's state," *IEEE Trans. Autom. Control*, vol. 58, no. 1, pp. 264–269, Jan. 2013.

[24] M. A. Henson and D. E. Seborg, "Time delay compensation for nonlinear processes," *Ind. Eng. Chem. Res.*, vol. 33, no. 6, pp. 1493–1500, Jun. 1994.

[25] J.-Q. Huang and F. L. Lewis, "Neural-network predictive control for nonlinear dynamic systems with time-delay," *IEEE Trans. Neural Netw.*, vol. 14, no. 2, pp. 377–389, Mar. 2003.

[26] I. Chakraborty, S. Obuz, R. Licitra, and W. E. Dixon, "Control of an uncertain Euler-Lagrange system with known time-varying input delay: A pde-based approach," in *Proc. Amer. Control Conf. (ACC)*, Jul. 2016, pp. 4344–4349.

[27] S. Obuz, J. R. Klotz, R. Kamalapurkar, and W. Dixon, "Unknown time-varying input delay compensation for uncertain nonlinear systems," *Automatica*, vol. 76, pp. 222–229, Feb. 2017.

[28] D. Bresch-Pietri and M. Krstic, "Delay-adaptive control for nonlinear systems," *IEEE Trans. Autom. Control*, vol. 59, no. 5, pp. 1203–1218, May 2014.

[29] A. Polyakov, D. Efimov, W. Perruquetti, and J.-P. Richard, "Output stabilization of time-varying input delay systems using interval observation technique," *Automatica*, vol. 49, no. 11, pp. 3402–3410, Nov. 2013.

[30] D. Bresch-Pietri and M. Krstic, "Adaptive trajectory tracking despite unknown input delay and plant parameters," *Automatica*, vol. 45, no. 9, pp. 2074–2081, Sep. 2009.

[31] D. Bresch-Pietri, J. Chauvin, and N. Petit, "Adaptive control scheme for uncertain time-delay systems," *Automatica*, vol. 48, no. 8, pp. 1536–1552, Aug. 2012.

[32] D. Enciu, I. Ursu, and G. Tecuceanu, "Dealing with input delay and switching in electrohydraulic servomechanism mathematical model," in *Proc. 5th Int. Conf. Control, Decis. Inf. Technol. (CoDIT)*, Apr. 2018, pp. 713–718.

[33] Y.-E. Wang, X.-M. Sun, and F. Mazenc, "Stability of switched nonlinear systems with delay and disturbance," *Automatica*, vol. 69, pp. 78–86, Jul. 2016.

[34] F. Mazenc, M. Malisoff, and H. Ozbay, "Stability analysis of switched systems with time-varying discontinuous delays," in *Proc. Amer. Control Conf.*, May 2017, pp. 5177–5181.

[35] M. Merad, R. J. Downey, S. Obuz, and W. E. Dixon, "Isometric torque control for neuromuscular electrical stimulation with time-varying input delay," *IEEE Trans. Control Syst. Technol.*, vol. 24, no. 3, pp. 971–978, May 2016.

[36] B. C. Allen, K. J. Stubbs, and W. E. Dixon, "Characterization of the time-varying nature of electromechanical delay during FES-cycling," *IEEE Trans. Neural Syst. Rehabil. Eng.*, vol. 28, no. 10, pp. 2236–2245, Oct. 2020.